Biotechnology and Bioprocess Engineering 28: 439-450 (2023)
DOI 10.1007/s12257-022-0256-9

pISSN 1226-8372
eISSN 1976-3816

RESEARCH PAPER

Decellularized Human Umbilical Artery Exhibits Adequate Endothelialization in Xenogenic Transplantation

Kai Hsia, Tien-Shiang Wang, Chin-Su Liu, Chih-Kuan Su, Chien-Chin Chen, Chang-Ching Yeh, Hsinyu Lee, Chao-Ling Yao, Tsung-Yu Tseng, Shih-Hwa Chiou, Hsu Ma, Chih-Hsun Lin, and Jen-Her Lu

Received: 31 August 2022 / Revised: 20 February 2023 / Accepted: 26 March 2023

Abstract Decellularized human umbilical arteries (dHUA) is an off-the-shelf graft that can potentially serve as vascular scaffolds in tissue engineering of small-diameter vascular grafts. This research aimed to investigate that dHUA could exhibit adequate endothelialization for a long term in xenogenic transplantation. 13 dHUAs were implanted in rat abdominal aortas up to 90 days. Rats were divided into three groups in terms of survival period: Group 1, one to seven days (n = 6); Group 2, 14 to 30 days (n = 4) and Group 3, 90 days (n = 3). The explants were analyzed by histological, immunohistochemistry and magnetic resonance angiography (MRA) examination. Allograft implantation of 12 decellularized rat abdominal aortas` were processed the same way as the rat in order to make a comparison for survival rates (Group 1, n = 5; Group 2, n = 4; Group 3, n = 3). The results demonstrated that the survival rates of xenograft and allograft implantation were estimated to be 59.2% *vs*. 58.3% in Group 1, 50.7% *vs*. 58.3% in Group 2 and 3. Grafts harvested from Group 2 were showed CD31, endothelial nitric oxide synthase expression at intima, and α-smooth muscle actin, CD45, CD68 and CD168 expression at the tunica externa. A layer structure with obvious endo-

Kai Hsia†, Shih-Hwa Chiou
Department of Medical Research, Taipei Veterans General Hospital, Taipei 11217, Taiwan

Tien-Shiang Wang†, Chih-Kuan Su†, Hsu Ma, Chih-Hsun Lin*
Division of Plastic and Reconstructive Surgery, Department of Surgery, Taipei Veterans General Hospital, Taipei 11217, Taiwan
Tel: +886-2-77370020; Fax: +886-2-77370023
E-mail: chlin12@vghtpe.gov.tw

Tien-Shiang Wang, Chin-Su Liu†, Hsu Ma, Chih-Hsun Lin
Department of Surgery, School of Medicine, National Yang Ming Chiao Tung University, Taipei 11221, Taiwan

Chin-Su Liu
Division of Transplantation Surgery, Department of Surgery, Taipei Veterans General Hospital, Taipei 11217, Taiwan

Chien-Chin Chen
Department of Pathology, Ditmanson Medical Foundation Chia-Yi Christian Hospital, Chiayi 600, Taiwan
Department of Cosmetic Science, Chia-Nan University of Pharmacy and Science, Tainan 717, Taiwan

Chang-Ching Yeh
Department of Obstetrics and Gynecology, Taipei Veterans General Hospital, Taipei 11217, Taiwan
Department of Obstetrics and Gynecology, National Yang Ming Chiao Tung University, Taipei 11221, Taiwan

Chang-Ching Yeh
Department of Nurse-Midwifery and Women Health, National Taipei University of Nursing and Health Sciences, Taipei 11219, Taiwan
Institute of Clinical Medicine, National Yang Ming Chiao Tung University, Taipei 11221, Taiwan

Hsinyu Lee
Department of Life Science, National Taiwan University, Taipei 10617, Taiwan

Chao-Ling Yao, Tsung-Yu Tseng
Department of Chemical Engineering, National Cheng Kung University, Tainan City 70101, Taiwan

Shih-Hwa Chiou
Institute of Pharmacology, National Yang Ming Chiao Tung University, Taipei 300093, Taiwan

Hsu Ma
Department of Surgery, School of Medicine, National Defense Medical Center, Taipei 11490, Taiwan

Jen-Her Lu*
Section of Pediatric Cardiology, Department of Pediatrics, Taipei Medical University Hospital, Taipei 11031, Taiwan
Tel: +886-2-77370020; Fax: +886-2-77370023
E-mail: jenherlu@gmail.com

†Kai Hsia, Tien-Shiang Wang, Chin-Su Liu, and Chih-Kuan Su contributed equally to this work as co-first authors.

thelialization and fiber regeneration/orientation could be inspected from the explants of Group 3. MRA demonstrated the patency of dHUA on day 30 and 90. In conclusion, more than 50% dHUA maintained patency in the xenogenic model till 90 days after surgery. A mature vessel-like functional structure with intact endothelial layer was observed then. This warrants further study in the reinforcement of decellularized vascular scaffolds.

Keywords: decellularization, human umbilical artery, xenogenic implantation endothelialization, magnetic resonance angiography

1. Introduction

With the urgent demand for biocompatible scaffold by tissue engineered vascular graft development, the potential of decellularized vascular graft has been proved in preclinical studies [1-4]. However, several clinical challenges such as thrombosis, intimal hyperplasia, aneurysm, rupture, immune rejection and calcification hinder its broad clinical applications. The mechanism associated with these sequelae in decellularized vascular graft is complicated and interrelated [5]. Improper decellularization protocol, immune response, and inflammatory reaction are thought to contribute to the failure mechanism. Suboptimal decellularization could result in structural instability and compliance mismatch, owing to microstructural alteration [6]. The inflammatory reaction against decellularized vascular scaffold *in vivo* is also thought to lead to graft failure.

The initial concern centers on the rejection reaction while using animal tissues as resources for decellularized scaffolds. However, current tissue processing methods can remove most antigens that induce host immune response toward extracellular matrix (ECM) scaffolds. A study evaluating biocompatibility in a dog model showed revitalization of the decellularized bovine scaffold (SynerGraft) with host smooth muscle cells, without aneurysm formation at 10-month follow-up [7]. Gui *et al*. [8] found that decellularized umbilical arterial scaffolds treated with CHAPS and sodium dodecyl sulfate (SDS) showed confluent endothelialization and significant smooth muscle cell infiltration in a nude rat model; however, some intimal hyperplasia was still noted after 8 weeks of implantation [8]. While reports have demonstrated aneurysm formation using SynerGraft for lower limb vascular bypass surgery, the histological examination of the explanted SynerGraft did not suggest hyper-acute immune response to the xenograft but simply an inflammatory response [9].

Incompetent mechanical properties of decellularized vascular scaffolds could also lead to dilatation or aneurysm formation. It has been shown that compliance of decellularized vascular scaffolds higher than native vessels dilates under pulsatile circulation [10]. Aneurysm formation could increase the risk of thrombosis and vessel rupture [11]. Tissue damage during decellularization or inflammatory degradation of scaffolds after implantation can result in changes in mechanical properties. Furthermore, the enzyme or detergents used for decellularization could lead to loss of collagen, elastin, and glycosaminoglycans, thereby impairing structural integrity [6]. After implantation, inflammation-mediated degradation of scaffold proteins by metalloproteinases (MMPs) can lyse major fibrous structures, weakening the scaffolds and leading to progressive aneurysmal dilatation [12].

We recently attempted to develop a decellularized human umbilical artery (dHUA) as a novel small-diameter vascular graft for clinical application because of the suitability of its size and ease of use. However, implantation of cell-free xenogenic, but not allogenic, vascular grafts in animal models has shown aneurysmal formation owing to the injury to the medial elastin and extracellular components within weeks [13]. Our preliminary magnetic resonance angiography (MRA) study also indicated aneurysmal dilatation of enzyme/detergent-treated porcine arterial scaffolds in a rat model at 30-day follow-up (unpublished data). Therefore, in this pre-clinical study, we investigated the *in vivo* performance of dHUA in a xenogenic implantation model. We hypothesized that an ideal decellularized scaffold will not elicit an aggressive inflammatory response or rejection and can be gradually transformed to the neovascular tissue in different species. We performed detergent-based decellularization of the human umbilical artery and evaluated the decellularization efficacy, biocompatibility and compliance of the scaffolds. The decellularized rat abdominal aorta (dRAA) acts as survival control. After the rat xenogenic transplantation, we surveyed endothelialization, collagen/elastin fiber regeneration, and cellular infiltration by histology of explanations from the three group of rats. We further investigated the patency and graft dilatation by MRA on day 30 and 90.

2. Materials and Methods

The study was approved by the Institutional Animal Care and Use Committee of Taipei Veterans General Hospital. All animal care complied with the Guide for the Care and Use of Laboratory Animals (No. 2018-265). Human tissue was obtained using protocols approved by the Institutional Review Board of Taipei Veterans General Hospital. All human subjects signed a consent form that was approved by the Institutional Review Board of Taipei Veterans

General Hospital (No. 2020-04-006C).

2.1. Resource of human umbilical artery and rat abdominal aorta

Human umbilical cords were obtained from the Department of Obstetrics and Gynecology at Taipei Veterans General Hospital. The cords were stored at 2-8°C immediately after delivery, and the overall storage time until processing in the laboratory did not exceed 24 h. Umbilical vessels approximately 20-30 cm long were isolated after meticulous removal of Wharton's jelly with sterile scissors. After dissection, two umbilical arteries were stored in phosphate-buffered saline (PBS, pH 7.4; Invitrogen) containing 250 μg/mL cefuroxime, 200 μg/mL ciprofloxacin, 80 μg/mL gentamicin, 50 μg/mL vancomycin, 1,000 units/mL colistin, and 200 μg/mL amphotericin B for 24 h at 4°C. Isolated umbilical arteries were then cut into approximately 5 cm long segments and flushed a few times with PBS. Umbilical arteries were either processed for histological analysis or prepared for decellularization.

The rat aorta was collected according to pervious description [14]. In brief, after the rats were anesthetized and incised along an abdominal midline, the aorta was identified and meticulously separated from the inferior vena cava in the retroperitoneal space. An intracardiac infusion of Lactated Ringer's solution (Y F CHEMICAL CORP.) with 10 U/mL heparin (China Biotech Corporation) was performed to flush blood out of the vessel. The aorta was harvested distally to the bifurcation followed by clamping the proximal end and ligating the branches. The disinfection treatment and storage of RAA were as same as HUA that was descripted above.

2.2. Decellularization of human umbilical artery and rat abdominal aorta

The decellularization protocol was performed according to our previous study for umbilical vein [15]. In brief, the segments of the umbilical artery were incubated in 0.1% SDS for 2 days, washed with PBS for another 2 days, and incubated with Medium 199 (Gibco) containing 12% fetal bovine serum for 2 days. The vessels were then washed with PBS. Decellularization was performed at 37°C on a shaker with 100 rpm agitation under sterile conditions. The treated arterial tissues were cryopreserved in −150°C liquid nitrogen using a computer control program and stored in the vapor phase of liquid nitrogen until use. The efficacy of decellularization was assessed by histological examination, DNA quantification, and mechanical testing. For evaluation of cellularity and histomorphology in decellularized vessels, approximately one cm long segments of native and decellularized umbilical arteries were fixed in 10% formaldehyde for 24 h and embedded in paraffin. Later, 5 μm thick transverse sections of the arteries were stained with hematoxylin and eosin (H&E; Sigma-Aldrich), 4′,6-diamidino-2-phenylindole (DAPI), Masson's trichrome, and Elastin Van Gieson (EVG) stains. DNA quantification was performed using the Quant-iT^{TM} PicoGreen® dsDNA reagent (Invitrogen) according to the manufacturer's instructions.

2.3. Evaluation of mechanical properties

The arterial grafts were tested at the maximum pressure of the system (200 mmHg). Vessels were attached to a flow circuit, submerged in and perfused with medium, and stretched to $\lambda = 1.3$ (130% of length prior to attachment). Luminal pressure was cycled between zero and a target pressure, which was incrementally increased by 10 mmHg after three cycles to each target (rate of increase ~60 mmHg/min and a rate of decrease of ~40 mmHg/min). The pressure was dynamically controlled using a sphygmomanometer while the vessel diameter was observed via light

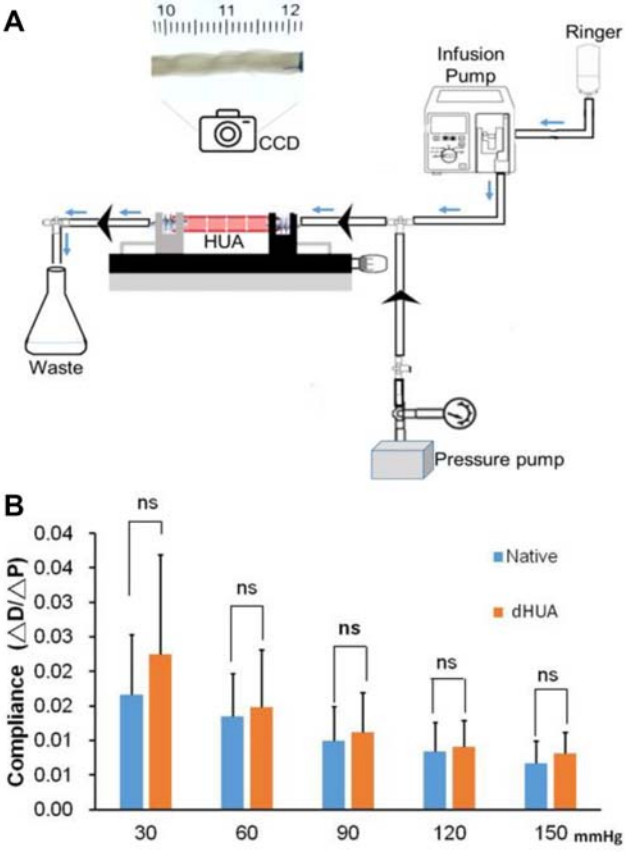

Fig. 1. Mechanical characterization of dHUA. (A) Mechanical property testing device utilized for assessing the vascular compliance. Arrow head implies air pressure flow, blue arrow indicates the direction of sheath flow. (B) Compliances of native HUA and dHUA at pressure from 30-150 mmHg. The result indicated that there was no significant different between Native HUA and dHUA ($p > 0.05$). Compliance = $\Delta D/\Delta$ ($\lambda = 1.3$). n = 3. dHUA: decellularized human umbilical artery.

microscopy, with images of the external diameter recorded and the diameter measured synchronously with pressure (Fig. 1A). Pressure-diameter data were used to determine the elastic recovery and compliance of the arteries and constructs. The mean diameter was calculated along a portion of the vessel length from the image data. Compliance was defined as the inverse of Peterson's elastic modulus according to the following equation: $C = (\Delta D/D0)/\Delta P$. Three arteries from each group were tested separately.

2.4. Biocompatibility test

To determine whether the dHUA could support cell colonization, Human umbilical vein endothelial cell (HUVEC), human cord blood-derived endothelial progenitor cells (EPC) and rat adipose stem cells (rASC) were seeded on the grafts *in vitro*. Cells were pre-stained with CellTracker™ CM-Dil (Thermo Fisher) according to instruction of manufacturer before seeding on the dHUA. In brief, we incubated cells in CM-Dil solution at a concentration of 1 ug/mL for 5 min at 37°C, subsequently moved the cells to 4°C fridge for additional 15 min to allow the dye to label the plasma membrane. The dye-labeled cells were washed with PBS and resuspended with culture medium. One cm dHUA was cut along long axis, spread out and put evenly on the bottom of 6-well plate with the luminal surface upside. 2×10^5 HUVEC, EPC and rASC were seeded on the segments respectively and incubated at 37°C, 5% CO_2 for 24 h. All samples were imaged under 100× and 200× magnification of confocal fluorescence microscopy (Zeiss LSM900; Imaging Core Facility of National Yang Ming Chiao Tung University). Seven fields of 100× magnification images of each group of samples were analyzed with Image J software (version 1.47). All fluorescence signal equal to or higher than background was regarded as a region of interest.

2.5. Implantation of vascular scaffolds in rat abdominal aorta

The cryopreserved dRAA and dHUA were defrozen in 37°C water bath before implantation. In total, thirteen male Sprague-Dawley (SD) rats (300-600 g; BioLASCO) received dHUA and twelve male SD rats received dRAA as an abdominal aorta bridge. Briefly, the rats were anesthetized with an intraperitoneal injection of 50 mg/kg body weight Zoletil 50 (Virbac). The anesthetized rats were then placed in a supine position over a warm pad. After shaving and sterilization, a midline laparotomy was performed. Then, the abdominal aorta between the infrarenal artery and iliac artery bifurcation was explored after lateralizing of the intestine and opening of the retroperitoneal fascia. The aorta was carefully dissected from the inferior vena cava, and the side branches were ligated. After clamping proximally and distally, the 1-cm aorta segment was replaced with grafts with end-to-end anastomosis (9-0 nylon, interrupted sutures). No anticoagulation or antiplatelet drugs were perioperatively administered. After the clamps were released, the hemostasis was checked, the visceral organs were returned, and the wound was closed in layers. The rats were anesthetized in a separate cage where they received food and water *ad libitum*. The animals were observed daily after operation.

2.6. Magnetic resonance angiography monitoring

Rats with graft implantation underwent MRA to evaluate the patency of the vascular graft on day 30 and 90. Imaging was performed using a 4.7-T magnetic resonance scanner (Biospec 47/40; Bruker BioSpin) equipped with an active shielding gradient (20 G/cm in 80 L). The rats were initially anesthetized with 5% isoflurane in air at a flow rate of 1 L/min. When fully anesthetized, the animals were placed in a prone position and fitted with a custom-designed head holder inside the instrument. Anesthesia was then maintained with 1.0-1.2% isoflurane in air at a flow rate of 1 L/min throughout the experiment. Images were acquired using a 72-mm birdcage transmitter coil and a separate quadrature surface coil for signal detection. T2WIs were acquired using a three-dimensional fast spin echo sequence as per the following parameters: repetition time, 2,200 ms; effective echo time, 33 ms; nex, 4; slice number, 20; slice thickness, 1.5 mm; matrix size, 200 × 200; field of view = 8.5 × 8.5 cm; scan time, 3 min.

2.7. Histological examination of implanted grafts

Histological examination was done on all implanted dHUA 7, 30 and 90 days after surgery if survived. Otherwise, necropsy was done for rats died unexpectedly. The procedure of explantation was the same as above under anesthesia. All the grafts were embedded in paraffin after fixation and dehydration. Four μm-thick transverse sections from the midportion segments of the grafts were stained with H&E, EVG, Masson's trichrome and immunohistochemistry (IHC) staining. Endothelialization was detected by H&E (Sigma-Aldrich), anti-CD31 (Abcam, ab182981, 1:200). Regeneration of ECM such as collagen and elastin was evaluated with Masson's trichrome and EVG staining. Anti-alpha-smooth muscle actin (Sigma-Aldrich, C6198, 1:5,000), Anti-CD68 (Abcam, ab31630, 1:80), Anti-CD163 (Abcam, ab182422, 1:1,000), and Anti-CD45 (Abcam, ab10558, 1:50) were used to investigate cellular infiltration. And an antibody for detecting endothelial nitric oxide synthase (eNOS; Abcam, ab5589, 1:80) was applied to identify functional endothelial cell. The HRP/DAB immunohistochemistry was performed on an automated IHC staining system noted as the Bond-MAX system (Leica Biosystems) with the Bond Polymer Refine Detection Kit (Leica). Images were captured with a

ZEISS inverted microscope. CD45, CD68 and CD163 positive cell and total cell number were quantified by Image J, the positive percentage was recorded. For each slide, ten images of 100× magnificent were taken for performing statistical analysis.

2.8. Statistical analysis

The data were shown as the mean ± standard deviation. Statistical analysis was performed using IBM SPSS Statistics 19 (version 19; SPSS). The Mann-Whitney *U*-test was done between experimental groups where $p < 0.05$ was considered significant. The Kruskal-Wallis test with post hoc Mann-Whitney *U*-test was used to compare data for more than two groups where $p < 0.05$ was considered significant.

3. Results

3.1. Characterization of dHUA

The dHUA maintained a tubular structure without fragility or collapse. The appearance of dHUA became whitish after decellularization. The diameter of dHUA was approximately 1.5-2 mm, which is slightly larger than that of the rat abdominal aorta (approximately 1-1.5 mm in diameter). As shown in Fig. 2, H&E staining revealed that most of the nuclear components in dHUA (Fig. 2E) were removed as compared with those in HUA (Fig. 2A). This result was further confirmed by DAPI staining (Fig. 2B and 2F). Masson's trichrome staining showed preservation of most collagenous components after decellularization (Fig. 2C and 2G). EVG staining indicated the preservation of small amounts of elastin fibers in the media layer (Fig. 2D and 2H). DNA content of native HUA was 392.46 ± 35.3 ng/mg while dHUA was 6.18 ± 3.2 ng/mg. DNA quantification revealed that more than 90% of dsDNA was eliminated from HUA. The biocompability was further verified by seeding HUVEC, EPC, and rASC onto grafts. After 24-hour-cultivation, the recellularized dHUA was examined using confocal microscopy, and cell attachment was quantified by the Image J software. Three types of cells show firm attachment on the lumen surface of dHUA with the area of

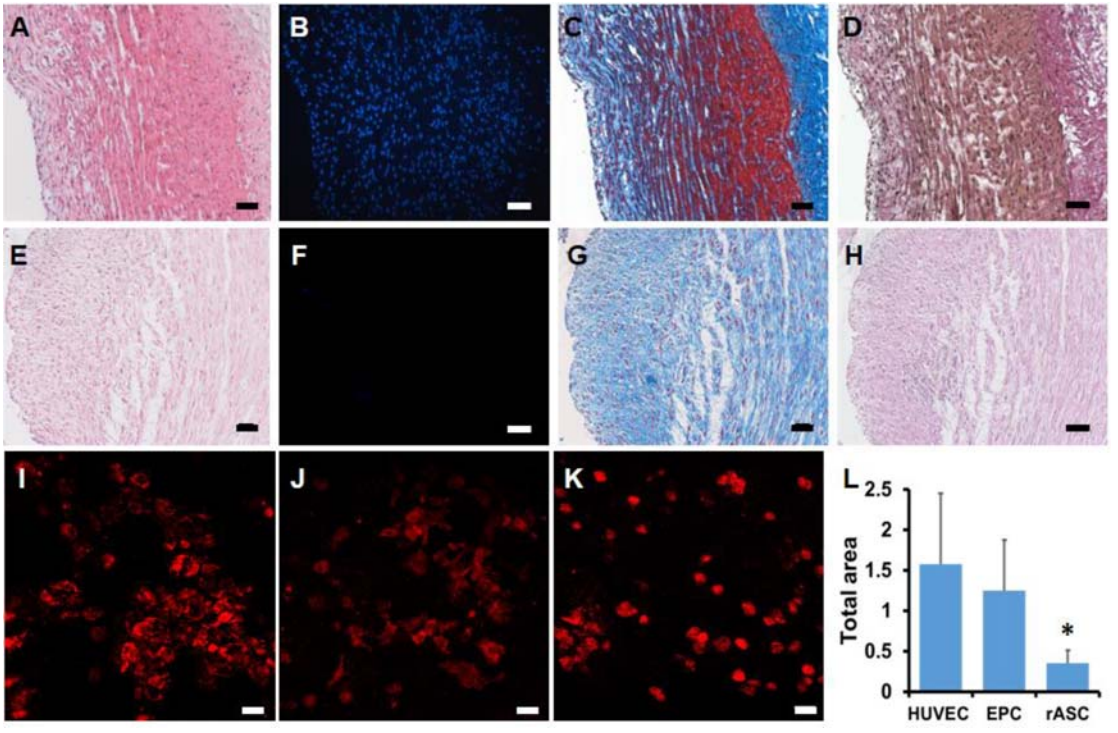

Fig. 2. Evaluation of the decellulariation efficacy and biocompability with histology, DNA, and cell ingrowth images of dHUA. (A) H&E of HUA; (B) DAPI of HUA; (C) Masson's trichrome stain of HUA; (D) Elastin Van Gieson stain of HUA; with histologicalstaining of (E) H&E of dHUA; (F) DAPI of dHUA; (G) Masson's trichrome stain of dHUA; (H) Elastin Van Gieson stain of dHUA. Magnification: 200×, Scale bar = 5 μm. Three types cells pre-labeled with CellTracker™ CM-Dil were grew on the lumen of dHUV for 24 h *in vitro*. (I) CM-Dil labeled HUVEC on dHUA; (J) CM-Dil labeled endothelial progenitor cell on dHUA and (K) CM-Dil labeled rASC on dHUA; (L) The area of cells labeled with red fluorescence presented by ROI. The result demonstrated that the dHUV was suitable for cell growth. The reason that the area of rASC was significantly smaller HUVEC and EPC was due to the rat cell was smaller than that of human. *$p < 0.05$, n = 5. dHUA: decellularized human umbilical artery, H&E: hematoxylin and eosin, DAPI: 4′,6-diamidino-2-phenylindole, rASC: rat adipose stem cell, ROI: region of interest, EPC: endothelial progenitor cell.

14.67 ± 5.7, 10.68 ± 5.4 and 3.01 ± 1.3 per field, respectably. The value of rASC was significantly lower than HUVEC and EPC because the rat cell was much smaller than that of human. These results indicated that dHUA were suitable for both allogeneic cell and xenogeneic cell growth (Fig. 2I, 2J, 2K, and 2L). Three vessels from each group were assembled on mechanical property testing device and measured individually. The vascular compliance did not show any significant difference between dHUA and HUA at pressures of 30, 60, 90, 120, and 150 mmHg (Fig. 1B). It revealed that the procedure of decellularization did not destroy the vascular structure notably.

3.2. Rat survival rate and graft diameter measurement

The dHUA was implanted into the rat abdominal aorta to test its *in vivo* biocompatibility. Compared with the diameter of dHUA while implanting in rats (Fig. 3), the implanted dHUA enlarged obviously under the observation of gross appearance on day 7 (Fig. 3A *vs*. 3B), day 30 (Fig. 3C *vs*. 3D) and day 90 (Fig. 3E *vs*. 3F). Evaluation of diameter change revealed the gradual increase in the diameter of dHUA by approximately 610%, 71% and 120% over 7, 30 and 90 days, respectively (Fig. 3G). At the initial stage of the operation, two rats died within 1 day owing to thrombosis (Fig. 4A). One rat was sacrificed on day 1, three rats died within 1 week and one died within 2 weeks, respectively. Six rats survived over 14 days and could survive up to 90 days. The 90-day survival rate was approximately 53.8% (7/13), as shown in Fig. 3H. The leading causes of unexpected death before day 7, especially on day 1, was thrombus formation and occlusion of the lumen that was revealed by histology. The diameter increased remarkably due to the vascular obstruction. Similarly, when dRAA was processed, five rats died within seven days due to thrombosis. Seven rats were alive until 90 days with survival rate of 58%. Based on our experiment, abdominal aorta occlusion caused the death of rat after operation. If we measure the patency of substitutes by survival rate, then more than 50% dHUA maintained patency in the xenogenic model till 90 days after surgery. Although the survival rate was lower

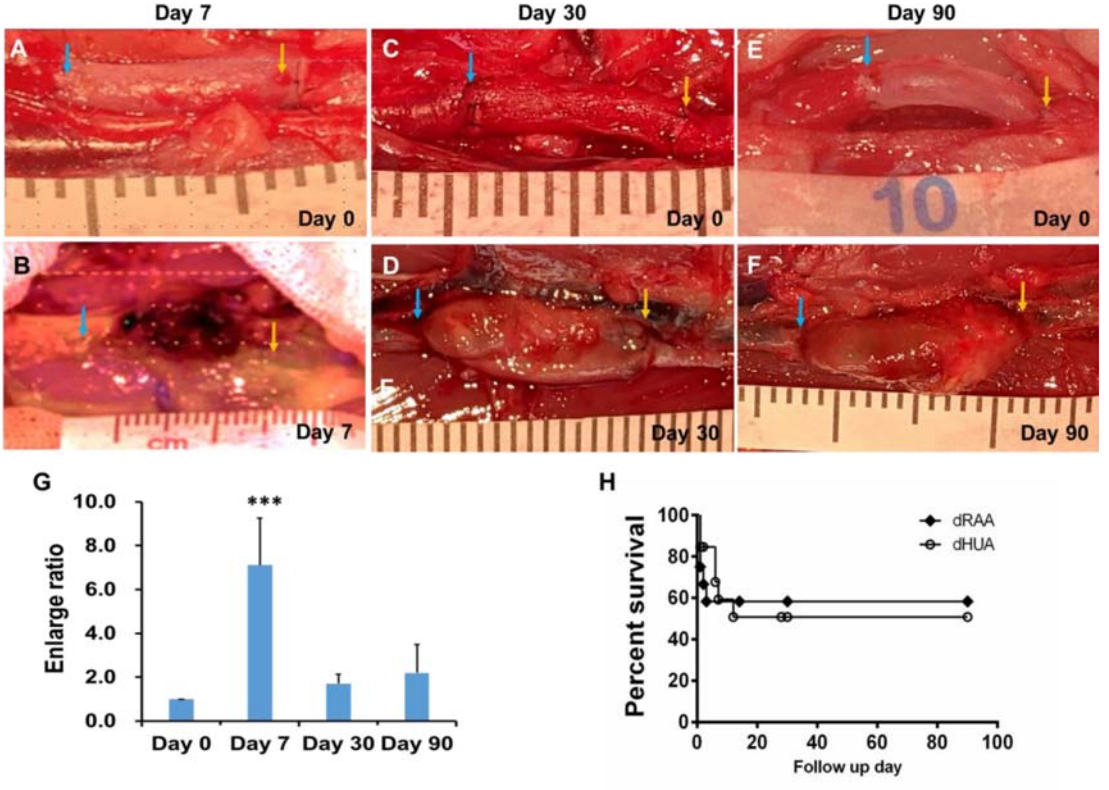

Fig. 3. Graft implantation of dHUA to rat aorta. (A-F) Gross appearance of the grafts at day of implantation (upper images) and harvest (lower images); (A) and (B) point to the rat at the time of operation and then harvested at day 7; (C) and (D) point to the rat at the time of operation and then harvested at day 30; (E) and (F) point to the rat at the time of operation and then harvested at day 90. Arrow: anastomosis, blue: near the head, yellow: near the tail; (G) The diameter enlargement ratio of day 7 was significantly larger than that of day 30 and day 90. The diameter of day 90 was larger than that of day 30, but no statistical significance. This means the dHUA enlarge immediately after anastomosis. (H) The survival curve of dRAA and dHUA implanted to rat aorta up to 90 days. dHUA: decellularized human umbilical artery, dRAA: decellularized rat abdominal aorta. ***$p < 0.001$.

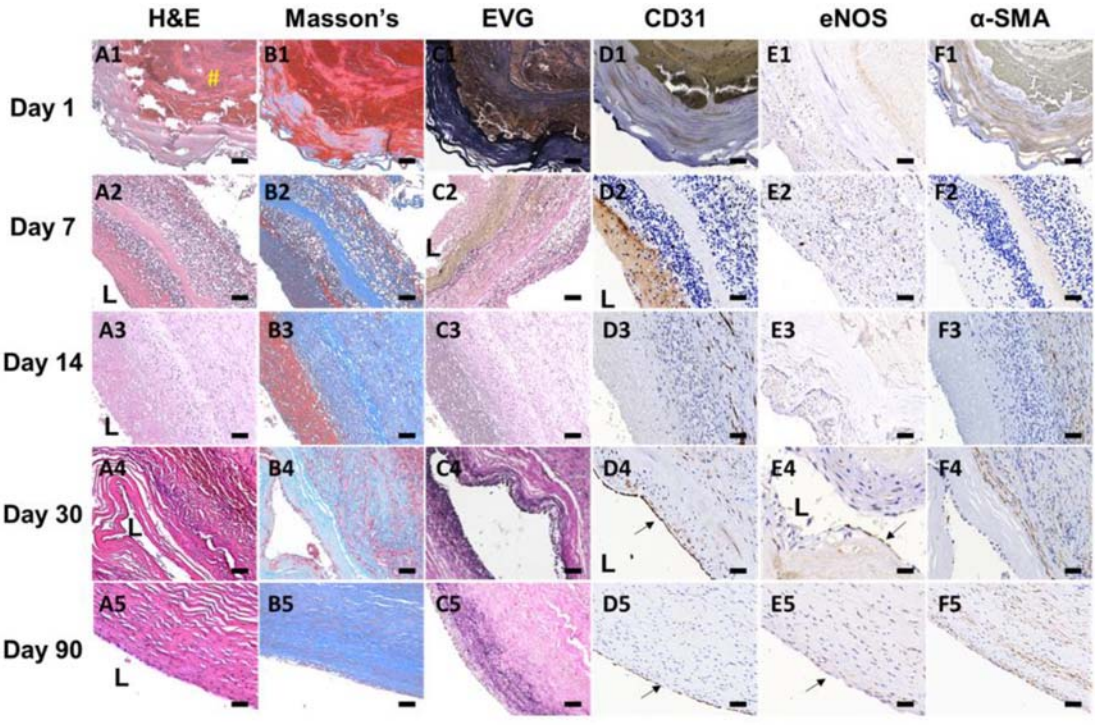

Fig. 4. Histological and immunochemistry staining of explant dHUA at day 1, 7 and 14. (A1-F1) Day 1; (A2-F2) Day 7; (A3-F3) Day 14; (A4-F4) Day 30; (A5-F5) Day 90; (A1-A5), H&E stain; (B1-B5) Masson's trichrome stain; (C1-C5) Elastin Van Gieson stain; (D1-D5) CD 31; (E1-E5) eNOS; (F1-F5) α-SMA. Magnification: 200×, Scale bar = 5 μm. Yellow hashtag points to thrombosis in lumen at Day-1. Black arrow indicates the endothelial layer stained by either CD31 or eNOS. L means the vascular lumen. dHUA: decellularized human umbilical artery, H&E: hematoxylin and eosin, eNOS: endothelial nitric oxide synthase, α-SMA: alpha-smooth muscle actin.

than allogenic implantation in the three groups, the rats would stay alive once they pull through the first 14 days post-surgery.

3.3. Collagen and elastin fiber regeneration

As shown in Fig. 4, on day one after the operation, thrombotic occlusion was observed in the aortic lumen of the dead rats, suggesting thrombosis as the cause of death (Fig. 4A1-4C1). Masson's trichrome staining demonstrated that collagen fibers in the tunica media of dHUA started to expose on day 7 (Fig. 4B2) and gradually increase on day 14 (Fig. 4B3), but no proliferative elastin fibers were observed in the tunica intima following EVG staining (Fig. 4C2 and 4C3). On day 30, persistent collagen fiber in the tunica media and proliferative elastin fibers at the tunica intima were observed (Fig. 4B4-4C4). On day 90, a mature layered structure with wavy collagen fibers in the tunica media and proliferative elastin fibers at the tunica intima was observed (Fig. 4B5-4C5).

3.4. Endothelialization of explanted grafts

In order to trace the endothelial cell on the lumen of the implanted scaffold, CD31, and eNOS were stained. No endothelial cells were noted on the inner surface of the grafts on day 1 and day 7 (Fig. 4D1-4E1 and 4D2-4E2). On day 14, $CD31^+$ (Fig. 4D3-4E3) were observed but intimal thickening with trace endothelialization was noted. On day 30, obvious endothelial cells were observed on the luminal side of the dHUA (Fig. 4A4) along with $CD31^+$ (Fig. 4D4). On day 90, more complete endothelialization (Fig. 4A5) and $CD31^+$ (Fig. 4D5) cells at the luminal side of the dHUA were noted. eNOS staining showed positive cells at the luminal side of the dHUA at day 30 and day 90 (Fig. 4E4 and 4E5). No obvious smooth muscle cells were illustrated in the grafts on day 1, 7, and 14 (Fig. 4F1-4F3) until 30 days and 90 days (Fig. 4F4 and 4F5). These findings demonstrated that the intact structure of graft with cells including endothelial cell and smooth muscle cell were assembled start 30 days and smooth muscle fascicles were more obvious on day 90 after dHUA implantation.

3.5. Cellular infiltration and degradation

No $CD45^+$, $CD68^+$, or $CD163^+$ lymphocytes were detected on day one (Fig. 5A, 5F, and 5K). It suggested that the reason of death in the acute stage was thrombosis instead of inflammation. With time went on, prominent $CD45^+$ and $CD68^+$ lymphocytes infiltration at media and outer layer was observed on day 7 (Fig. 5B and 5G). The number of

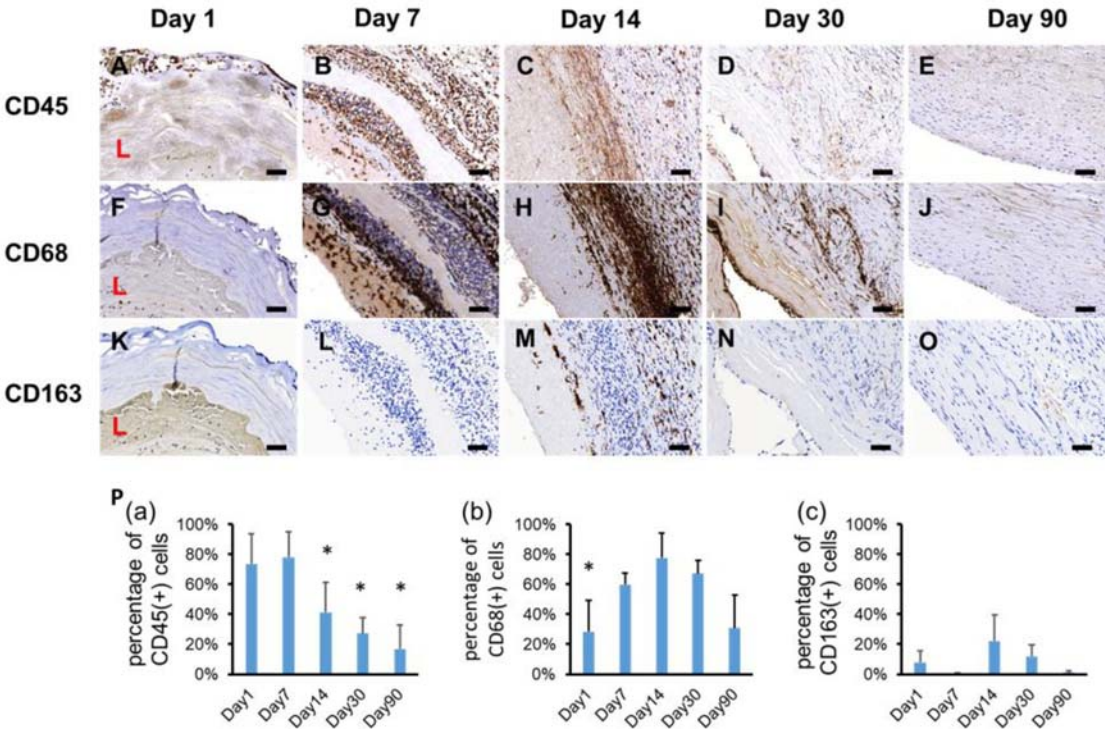

Fig. 5. Immunochemistry staining of explant dHUA at day 1, 7, 14, 30, 90 after surgery. (A, F, K) Day 1; (B, G, L) Day 7; (C, H, M) Day 14; (D, I, N) Day 30; (E, J, O) Day 90; (A-E) CD45; (F-J) CD68; (K-O) CD163; Magnification: 200×, Scale bar = 5 μm. (P) Quantification of IHC stain of explant dHUA at day 1, 7, 14, 30, 90. (a) CD45; (b) CD163; (c) CD68. n = 13. Red L means the vascular lumen. dHUA: decellularized human umbilical artery, IHC: immunohistochemistry. * $p < 0.05$.

$CD45^+$, $CD68^+$ and $CD163^+$ cells reached a high level on day 14 (Fig. 5C, 5H, and 5M). Persistent but less $CD68^+$ cell infiltration in the outer layer and fewer $CD45^+$, $CD163^+$ cells were noted on day 30 (Fig. 5D, 5I, and 5N). No obvious $CD45^+$, $CD68^+$, or $CD163^+$ cells were detected in the tunica media on day 90 (Fig. 5E, 5J, and 5O). The percentage of semi-quantified $CD45^+$, $CD68^+$, and $CD163^+$ cells are shown in Fig. 5P. On day 7, and 14, most infiltrated cells were lymphocytes and $CD68^+$ macrophages; the cell count gradually decreased at day 30 and 90. $CD163^+$ cells were noted on day 14. It revealed that the inflammatory reaction happened from day 7 and became serious at day 14. Once the animal passed through this critical stage, the inflammatory alleviated and the animal would survive.

3.6. Results of MRA

As shown in Fig. 6, MRA images revealed the patency of dHUA in the rat abdominal aorta on day 90. However,

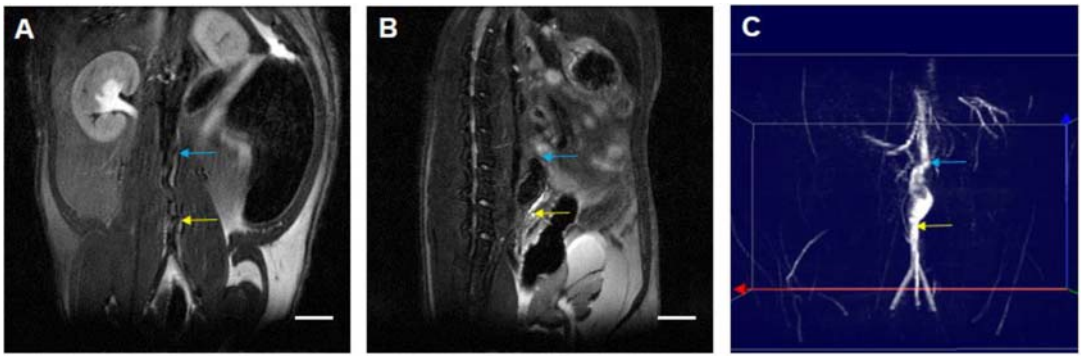

Fig. 6. MRA images of implanted dHUA at day 90. (A) T2 image of the coronal view of implantation graft in rat abdominal cavity; (B) T2 image of the sagittal view of implantation graft in rat abdominal cavity; (C) TOF 3D display of the abdominal artery with the implantation graft. Scale bar = 1 cm. Arrow: anastomosis, blue: near the head, yellow: near the tail. MRA: magnetic resonance angiography, dHUA: decellularized human umbilical artery, TOF: time of flight, 3D: three-dimensional.

graft dilatation was obvious in comparison with the rat aorta. The result showed that the dHUA was enlarged even the rats were alive. It hinted that the mechanical property of dHUA needed strengthen in order to tolerate long-term blood pressure *in vivo*.

4. Discussion

Aneurysmal dilation has been associated with the failure mechanism in vascular ECM scaffolds. Aneurysm formation results in turbulent blood flow and increases the risk of thrombosis and vessel rupture, owing to the increased wall stress at the aneurysmal site [5]. Gui *et al*. [8] reported distention of decellularized umbilical arteries to approximately 4.5 mm (diameter) immediately upon implantation in nude rat abdominal aortas. These authors primarily used SDS, CHAPS, and serum for the decellularization of umbilical arteries and found that most of the elastin was removed and collagen was preserved. The initial dilatation could be attributed to the loss of elastin in the scaffolds. At 8 weeks, no obvious dilation or aneurysm formation was reported. However, ultrasound revealed disturbed flow near the anastomosis region and a significantly lower flow rate in the graft than in the native aorta [8]. These results differed from our findings. We did not observe dilatation immediately after implantation, although a slight diameter mismatch existed. These differences could be from the variations in decellularization protocols and animal models. In our study, no obvious gross dilatation of dHUA was observed till 14 days after surgery. It occurred on day 30 to be observable via gross examination and MRA. These findings support that dHUA could maintain the blood flow in the rat aorta, but the risk of graft dilatation cannot be eliminated. MRA confirmed patency along with the slight decrease in flow rate as compared to that in the native artery.

Nevertheless, the histology on day one showed red blood cells at the vessel wall of dHUA, and this phenomenon was not reported in other studies. However, this abnormality resolved and was not observed on day 14. A possible explanation could be the damage to the microscopic vessel wall after decellularization, although the integrity of dHUA was evaluated by a perfusion mechanical test before implantation. It is known that the reagents used for decellularization can also affect the composition of tissues. The results indicated that grossly preserved collagen in dHUA could temporarily withstand the blood flow into the vessel wall [16,17]. Another explanation is that dHUA exhibit biological activity to absorb the extravasation of the blood and then undergo remodeling without total dissection or rupture.

Immunogenic reactions or inflammation is thought to be a cause of aneurysmal dilatation of decellularized vascular grafts *in vivo*. Allaire *et al*. [12] established an animal aneurysm model using xenogenic transplantation and showed that arterial wall degeneration and dilation result from the penetration of inflammatory cells into the media and upregulation of MMP expression. MMPs have been extensively studied in aneurysms because they can degrade most of the arterial ECM, including collagen and elastin [12]. In addition, histological examination of the explanted bovine ureter (SynerGraft) did not suggest any hyper-acute immune response to the xenograft but simply an inflammatory reaction. However, inflammatory reaction was expected and promoted by the manufacturer as a part of the revitalization process and was even observed at 13 weeks in a dog experiment [9]. As bench testing prior to implantation has confirmed the similar burst strength of the grafts and long saphenous vein, Cyolife Inc. hypothesized that it is the inflammatory response that is responsible for the weakening of the wall.

Although decellularization was meant to reduce the host immune response toward the ECM scaffold, it is rarely capable of completely eliminating it. Immune attacks from either natural or acquired antibodies can lead to the recruitment of both adaptive and innate immune cells [18]. Immune cell recruitment is further exacerbated by the presence of graft chemoattractants such as collagen fragments [19,20]. Antigen recognition and co-stimulation between cells result in increased secretion of cytokines and MMPs [21]. Aneurysm studies in humans have shown that monocyte-macrophages and T-lymphocytes are the sources of ECM-degrading enzymes, as they play key roles in the formation of atherosclerotic plaques and arthritic joints [22,23]. Cytokines further stimulate pro-inflammatory responses, cell recruitment, and MMP secretion [24]. Increased secretion of MMPs, as previously mentioned, leads to the degradation of structural proteins of the ECM scaffold and the consequent damage to the graft. The combined effect of immune activation results in the degradation of ECM proteins and scaffold failure by either or all of the aforementioned mechanisms [5].

Our findings depicted the *in vivo* changes in the decellularized vascular grafts in a xenogenic model. The dHUA provoked a mild inflammatory reaction, as evident from $CD45^+$ and $CD68^+$ cells at the early stage of implantation. The infiltration of $CD68^+$ cells was mainly noted in the adventitia and was recognized from host cells [25]. The exposure of the decellularized matrix to the blood leads to the release of chemokines/cytokines by activated platelets on the inner surface, eventually resulting in the recruitment of inflammatory cells or leukocytes [26,27]. It is known that macrophages are important in the degradation of ECM scaffolds and quickly populate the ECM *in vivo*. Macrophages also participate in scaffold remodeling [28,29] $CD68^+$ cells

have the ability to induce smooth muscle cell and endothelial cell incorporation in the graft [30]. We could not observe smooth muscle cell infiltration until day 14 after implantation. Smooth muscle cells infiltrating the neointima of decellularized vascular grafts could be derived from three cell types: cells from the surrounding tissue, those from the recipient arterial vessel wall, and those circulating in the blood. Progenitors from the neointima of decellularized vascular grafts also have the ability to differentiate into smooth muscle cells [31]. However, smooth muscle cells are recognized to contribute to neointimal hyperplasia, which was observed to some extent in dHUA on day 1, 7, and 14 in the present study. Endothelial cells appeared on the inner surface of dHUA on day 14, and this phenomenon was accompanied by persistent infiltration of macrophages and smooth muscle cells. This could be explained by the fact that the degradation of the ECM by inflammatory cells can release many matricryptic molecules. These bioactive molecules have chemoattractant effects on stem and endothelial cells [32]. Similar to smooth muscle cells, endothelial cells on decellularized vascular grafts could be derived from transanastomotic growth, transmural growth, and recruited circulating blood cells by factors released from degraded scaffolds [33]. Roh *et al*. [30] also showed that tissue-engineered vascular grafts could transform into functional neo-vessels via inflammatory processes, mainly monocyte activation. In addition, Kristofik *et al*. [34] suggested that the appearance of $CD68^+$ cells in ECM-incorporated decellularized vascular grafts could have certain advantages in endothelial cell recruitment. In our analysis, lymphocytes infiltrated the grafts early after implantation. The number of CD68 macrophages gradually increased from day 1 to 14 and decreased thereafter. The number of CD163 macrophages was found to be low, indicating that the inflammatory reaction was only temporary and that the degradation of scaffolds was mild and accompanied by regeneration of matrix proteins. The M1 to M2 macrophage transition is important for ECM-based scaffolds, but we did not observe this phenomenon [35].

To avoid aneurysm formation, it is imperative to prevent ECM injury during decellularization. Non-detergent or non-enzyme methods are continuously being explored for decellularization of vascular tissues to avoid harmful effects. For example, high hydrostatic pressure has been reported to almost completely remove the cellular components of porcine arteries without any obvious change in elastic modulus [36]. Ultrahigh hydrostatic pressure-treated scaffolds maintained the ECM and facilitated peptide immobilization on the luminal surface, thereby inducing rapid endothelialization *in vivo* [37]. Another approach of preventing aneurysm is decrease the inflammation of scaffolds *in vivo* by preliminary seeding cells (recellularization). The advantages of recellularization of decellularized scaffolds before implantation include physical mask or degradation of antigen by the cells and reduced coagulation cascade [38]. However, there are major hurdles to be circumvented, such as selection of cell source and type, differentiation or stemness, seeding number, and efficacy of recellularization [39]. The addition of other degradable biomaterials to decellularized vascular scaffolds might compensate for the altered mechanical properties during decellularization treatment [40,41].

In order to explore the long term outcomes of the vascular xenotransplantation, 90-days-long after surgery was used to estimate. Based Andreollo *et al*.'s [42] conclusion in the review article, every month of an adult rat is almost equal to 2.5 human years. Therefore, 90 days for rat is roughly equivalent to six to eight years for human life. It would be long enough to evaluate the biological and physiological behavior of the implanted vessel, and the possible causes of failure as well. We also found that in the images of IHC staining, thick brown areas were observed to be a thinner layer in the samples which might be nonspecific interference due to the blood infiltration to explants. The residue blood was difficult to be eliminated because some samples harvested from the cadavers whose blood has clotted. The immunofluorescence staining could be employed to overcome the bias.

5. Conclusion

We observed that the dHUA was a xenogenic small-caliber vascular graft that could maintain the blood flow for up to 90 days *in vivo*. Although dilatation of the graft and possibility of graft failure still exist, the functionalization of the dHUA could be derived from its ability to endothelialize, evoke cellular infiltration, and elicit a low-grade inflammatory reaction. Endothelialization could be observed on day 30 after implantation. Regeneration of collagen/elastin and increase in cellularity were noted thereafter. Although a mature vessel-like functional structure was observed on day 90, the dilatation of dHUA was noted.

Acknowledgements

This work was supported by grants R16001 and R16002 from I-MEI FOODS CO., LTD, and Taipei Veterans General Hospital. We thank the Taiwan Mouse Clinic, Academia Sinica and Taiwan Animal Consortium for the technical support in MRA.

Funding

This research received funding support from the Taiwan Ministry of Science and Technology, MOST107-2314-B-075-030, 108-2314-B-075-053, 108-2314-B-075-045, 108WHA0110304, 109WHA0110184, and MOST 109-2314-B-038-143.

Author's Contributions

Kai Hsia: Methodology, Data curation, Writing—Original draft preparation & editing. Tien-Shiang Wang: Data curation, Review and editing. Chin-Su Liu: Investigation, Writing—Review and editing. Chih-Kuan Su: Methodology, Original draft preparation. Chien-Chin Chen: Pathology. Chang-Ching Yeh: Sample collection and preparation. Hsinyu Lee: Supervision. Chao-Ling Yao: Supervision. Tsung-Yu Tseng: Administration. Shih-Hwa Chiou: Supervision, Review and editing. Hsu Ma: Supervision. Chih-Hsun Lin: Methodology, Writing—Original draft preparation. Jen-Her Lu: Reviewing and editing, Funding acquisition, Conceptualization and supervision.

Ethical Statements

The authors declare no conflict of interest.
The study was approved by the Institutional Animal Care and Use Committee of Taipei Veterans General Hospital. All animal care complied with the Guide for the Care and Use of Laboratory Animals (No. 2018-265). Human tissue was obtained using protocols approved by the Institutional Review Board of Taipei Veterans General Hospital. All human subjects signed a consent form that was approved by the Institutional Review Board of Taipei Veterans General Hospital (No. 2020-04-006C).

References

1. Ma, X., Z. He, L. Li, G. Liu, Q. Li, D. Yang, Y. Zhang, and N. Li (2017) Development and *in vivo* validation of tissue-engineered, small-diameter vascular grafts from decellularized aortae of fetal pigs and canine vascular endothelial cells. *J. Cardiothorac. Surg*. 12: 101.
2. Kaushal, S., G. E. Amiel, K. J. Guleserian, O. M. Shapira, T. Perry, F. W. Sutherland, E. Rabkin, A. M. Moran, F. J. Schoen, A. Atala, S. Soker, J. Bischoff, and J. E. Mayer Jr. (2001) Functional small-diameter neovessels created using endothelial progenitor cells expanded *ex vivo*. *Nat. Med.* 7: 1035-1040.
3. Tillman, B. W., S. K. Yazdani, L. P. Neff, M. A. Corriere, G. J. Christ, S. Soker, A. Atala, R. L. Geary, and J. J. Yoo (2012) Bioengineered vascular access maintains structural integrity in response to arteriovenous flow and repeated needle puncture. *J. Vasc. Surg*. 56: 783-793.
4. Neff, L. P., B. W. Tillman, S. K. Yazdani, M. A. Machingal, J. J. Yoo, S. Soker, B. W. Bernish, R. L. Geary, and G. J. Christ (2011) Vascular smooth muscle enhances functionality of tissue-engineered blood vessels *in vivo*. *J. Vasc. Surg.* 53: 426-434.
5. Lopera Higuita, M. and L. G. Griffiths (2020) Small diameter xenogeneic extracellular matrix scaffolds for vascular applications. *Tissue Eng. Part B Rev.* 26: 26-45.
6. Williams, C., J. Liao, E. M. Joyce, B. Wang, J. B. Leach, M. S. Sacks, and J. Y. Wong (2009) Altered structural and mechanical properties in decellularized rabbit carotid arteries. *Acta Biomater.* 5: 993-1005.
7. Clarke, D. R., R. M. Lust, Y. S. Sun, K. S. Black, and J. D. Ollerenshaw (2001) Transformation of nonvascular acellular tissue matrices into durable vascular conduits. *Ann. Thorac. Surg.* 71(5 Suppl): S433-S436.
8. Gui, L., A. Muto, S. A. Chan, C. K. Breuer, and L. E. Niklason (2009) Development of decellularized human umbilical arteries as small-diameter vascular grafts. *Tissue Eng. Part A* 15: 2665-2676.
9. Sharp, M. A., D. Phillips, I. Roberts, and L. Hands (2004) A cautionary case: the SynerGraft vascular prosthesis. *Eur. J. Vasc. Endovasc. Surg*. 27: 42-44.
10. Towne, J. B. and L. H. Hollier (2004) *Complications in Vascular Surgery.* 2nd ed. CRC Press.
11. Quint, C., Y. Kondo, R. J. Manson, J. H. Lawson, A. Dardik, and L. E. Niklason (2011) Decellularized tissue-engineered blood vessel as an arterial conduit. *Proc. Natl. Acad. Sci. U. S. A.* 108: 9214-9219.
12. Allaire, E., R. Forough, M. Clowes, B. Starcher, and A. W. Clowes (1998) Local overexpression of TIMP-1 prevents aortic aneurysm degeneration and rupture in a rat model. *J. Clin. Invest*. 102: 1413-1420.
13. Allaire, E., C. Guettier, P. Bruneval, D. Plissonnier, and J.-B. Michel (1994) Cell-free arterial grafts: morphologic characteristics of aortic isografts, allografts, and xenografts in rats. *J. Vasc. Surg*. 19: 446-456.
14. Hsia, K., C. H. Lin, H. Y. Lee, W. M. Chen, C. L. Yao, C. C. Chen, H. Ma, S. J. Wang, and J. H. Lu (2019) Sphingosine-1-phosphate in endothelial cell recellularization improves patency and endothelialization of decellularized vascular grafts *in vivo*. *Int. J. Mol. Sci.* 20: 1641.
15. Hsia, K., M. J. Yang, W. M. Chen, C. L. Yao, C. H. Lin, C. C. Loong, Y. L. Huang, Y. T. Lin, A. D. Lander, H. Lee, and J. H. Lu (2017) Sphingosine-1-phosphate improves endothelialization with reduction of thrombosis in recellularized human umbilical vein graft by inhibiting syndecan-1 shedding in vitro. *Acta Biomater.* 51: 341-350.
16. Crapo, P. M., T. W. Gilbert, and S. F. Badylak (2011) An overview of tissue and whole organ decellularization processes. *Biomaterials* 32: 3233-3243.
17. Lin, C.-H., Y.-C. Kao, Y.-H. Lin, H. Ma, and R.-Y. Tsay (2016) A fiber-progressive-engagement model to evaluate the composition, microstructure, and nonlinear pseudoelastic behavior of porcine arteries and decellularized derivatives. *Acta Biomater.* 46: 101-111.
18. Morris, A. H., D. K. Stamer, and T. R. Kyriakides (2017) The host response to naturally-derived extracellular matrix biomaterials. *Semin. Immunol*. 29: 72-91.
19. Human, P. and P. Zilla (2001) Inflammatory and immune processes: the neglected villain of bioprosthetic degeneration? *J. Long Term Eff. Med. Implants* 11: 199-220.
20. Rieder, E., A. Nigisch, B. Dekan, M.-T. Kasimir, F. Mühlbacher, E. Wolner, P. Simon, and G. Weigel (2006) Granulocyte-based immune response against decellularized or glutaraldehyde cross-linked vascular tissue. *Biomaterials* 27: 5634-5642.
21. Goetzl, E. J., M. J. Banda, and D. Leppert (1996) Matrix metalloproteinases in immunity. *J. Immunol*. 156: 1-4.

22. Suma, H., T. Isomura, T. Horii, and T. Sato (2000) Late angiographic result of using the right gastroepiploic artery as a graft. *J. Thorac. Cardiovasc. Surg*. 120: 496-498.
23. Chiu, T. and A. Burd (2005) "Xenograft" dressing in the treatment of burns. *Clin. Dermatol.* 23: 419-423.
24. Courtman, D. W., B. F. Errett, and G. J. Wilson (2001) The role of crosslinking in modification of the immune response elicited against xenogenic vascular acellular matrices. *J. Biomed. Mater. Res.* 55: 576-586.
25. Valentin, J. E., N. J. Turner, T. W. Gilbert, and S. F. Badylak (2010) Functional skeletal muscle formation with a biologic scaffold. *Biomaterials* 31: 7475-7484.
26. Gawaz, M., H. Langer, and A. E. May (2005) Platelets in inflammation and atherogenesis. *J. Clin. Invest*. 115: 3378-3384.
27. McEver, R. P. (2001) Adhesive interactions of leukocytes, platelets, and the vessel wall during hemostasis and inflammation. *Thromb. Haemost.* 86: 746-756.
28. Valentin, J. E., A. M. Stewart-Akers, T. W. Gilbert, and S. F. Badylak (2009) Macrophage participation in the degradation and remodeling of extracellular matrix scaffolds. *Tissue Eng. Part A* 15: 1687-1694.
29. Wolf, M. T., K. A. Daly, E. P. Brennan-Pierce, S. A. Johnson, C. A. Carruthers, A. D'Amore, S. P. Nagarkar, S. S. Velankar, and S. F. Badylak (2012) A hydrogel derived from decellularized dermal extracellular matrix. *Biomaterials* 33: 7028-7038.
30. Roh, J. D., R. Sawh-Martinez, M. P. Brennan, S. M. Jay, L. Devine, D. A. Rao, T. Yi, T. L. Mirensky, A. Nalbandian, B. Udelsman, N. Hibino, T. Shinoka, W. M. Saltzman, E. Snyder, T. R. Kyriakides, J. S. Pober, and C. K. Breuer (2010) Tissue-engineered vascular grafts transform into mature blood vessels via an inflammation-mediated process of vascular remodeling. *Proc. Natl. Acad. Sci. U. S. A.* 107: 4669-4674.
31. Tsai, T.-N., J. P. Kirton, P. Campagnolo, L. Zhang, Q. Xiao, Z. Zhang, W. Wang, Y. Hu, and Q. Xu (2012) Contribution of stem cells to neointimal formation of decellularized vessel grafts in a novel mouse model. *Am. J. Pathol.* 181: 362-373.
32. Vorotnikova, E., D. McIntosh, A. Dewilde, J. Zhang, J. E. Reing, L. Zhang, K. Cordero, K. Bedelbaeva, D. Gourevitch, E. Heber-Katz, S. F. Badylak, and S. J. Braunhut (2010) Extracellular matrix-derived products modulate endothelial and progenitor cell migration and proliferation *in vitro* and stimulate regenerative healing in vivo. *Matrix Biol.* 29: 690-700.
33. Avci-Adali, M., G. Ziemer, and H. P. Wendel (2010) Induction of EPC homing on biofunctionalized vascular grafts for rapid *in vivo* self-endothelialization--a review of current strategies. *Biotechnol. Adv.* 28: 119-129.
34. Kristofik, N. J., L. Qin, N. E. Calabro, S. Dimitrievska, G. Li, G. Tellides, L. E. Niklason, and T. R. Kyriakides (2017) Improving *in vivo* outcomes of decellularized vascular grafts via incorporation of a novel extracellular matrix. *Biomaterials* 141: 63-73.
35. Badylak, S. F. (2014) Decellularized allogeneic and xenogeneic tissue as a bioscaffold for regenerative medicine: factors that influence the host response. *Ann. Biomed. Eng.* 42: 1517-1527.
36. Funamoto, S., K. Nam, T. Kimura, A. Murakoshi, Y. Hashimoto, K. Niwaya, S. Kitamura, T. Fujisato, and A. Kishida (2010) The use of high-hydrostatic pressure treatment to decellularize blood vessels. *Biomaterials* 31: 3590-3595.
37. Yamanaka, H., T. Yamaoka, A. Mahara, N. Morimoto, and S. Suzuki (2018) Tissue-engineered submillimeter-diameter vascular grafts for free flap survival in rat model. *Biomaterials* 179: 156-163.
38. Robertson, M. J., J. L. Dries-Devlin, S. M. Kren, J. S. Burchfield, and D. A. Taylor (2014) Optimizing recellularization of whole decellularized heart extracellular matrix. *PLoS One* 9: e90406.
39. Bilodeau, C., O. Goltsis, I. M. Rogers, and M. Post (2020) Limitations of recellularized biological scaffolds for human transplantation. *J. Tissue Eng. Regen. Med.* 14: 521-538.
40. Gong, W., D. Lei, S. Li, P. Huang, Q. Qi, Y. Sun, Y. Zhang, Z. Wang, Z. You, X. Ye, and Q. Zhao (2016) Hybrid small-diameter vascular grafts: anti-expansion effect of electrospun poly ε-caprolactone on heparin-coated decellularized matrices. *Biomaterials* 76: 359-370.
41. Negishi, J., Y. Hashimoto, A. Yamashita, Y. Zhang, T. Kimura, A. Kishida, and S. Funamoto (2017) Evaluation of small-diameter vascular grafts reconstructed from decellularized aorta sheets. *J. Biomed. Mater. Res. A* 105: 1293-1298.
42. Andreollo, N. A., E. F. Santos, M. R. Araújo, and L. R. Lopes (2012) Rat's age versus human's age: what is the relationship? *Arq. Bras. Cir. Dig.* 25: 49-51.